Novel Class of Neural Stochastic Resonance and Error-Free Information Transfer

Hideaki Yasuda,[1] Tsuyoshi Miyaoka,[1] Jun Horiguchi,[1] Akira Yasuda,[2] Peter Hänggi,[3] and Yoshiharu Yamamoto[4,*]

[1]*Department of Psychiatry, School of Medicine, Shimane University, 89-1 Enyacho, Izumo City, Shimane 693-8501, Japan*
[2]*Department of Medical Informatics, School of Medicine, Shimane University, 89-1 Enyacho, Izumo City, Shimane 693-8501, Japan*
[3]*University of Augsburg, Institute of Physics, Universitätsstrasse 1, D-86135 Augsburg, Germany*
[4]*Educational Physiology Laboratory, Graduate School of Education, The University of Tokyo, 7-3-1 Hongo, Bunkyo-ku, Tokyo 113-0033, Japan*

(Received 18 October 2007; published 19 March 2008)

We investigate a novel class of neural stochastic resonance (SR) exhibiting error-free information transfer. Unlike conventional neural SR, where the decrease of a system's response with too much noise is associated with an increase in the baseline firing rate, here the bell-shaped SR behavior of the input-output cross correlation emerges versus increasing input noise in spite of no significant increase of the baseline firing rate. The neuron thus acts as an error-free detector for weak signals. An integrate-and-fire model with short-term synaptic depression convincingly validates our experimental findings for SR in the human tactile blink reflex.

DOI: 10.1103/PhysRevLett.100.118103 PACS numbers: 87.19.lt, 05.40.Ca, 43.50.+y

Stochastic resonance (SR), the enhancement of information transfer through systems exhibiting nonlinearity by the addition of an optimal level of noise to the system in the presence of a small signal, is ubiquitous in nonliving and living systems [1–3]. In particular, this physical concept has greatly impacted neuroscience research because neurons or their assemblies, owing to their threshold-type nonlinearity, can exploit this mechanism to detect weak inputs. Indeed, SR has been demonstrated experimentally in many neural systems in animals [4–7] and humans [8–11].

To date, physical mechanisms of neural SR have typically been studied in the framework of noise-assisted and signal-dependent state transitions in monostable systems with a threshold or boundary [2,12], bistable systems [2], and excitable systems [13], as abstract models of single neurons or neural assemblies. In these systems, an optimal level of noise plays a constructive role in assisting the signal-dependent state transitions, or firings in the neural models, thus enhancing the input-output information transfer. With too much noise, however, increased random transitions or firings degrade the system's ability, leading to the characteristic, ''bell-shaped'' curve in the information transfer.

Here, we introduce a novel class of neural SR, where the decline of the bell-shaped curve for large input noise arises without any increase in noise-induced random firings. Because of this feature, the neuron can efficiently transfer information about weak input signals without erroneous firings, even when exposed to a noisy environment. As a first experimental realization, we explore the tactile blink reflex in humans: the ability of air-puff stimulations to an eyelid (input) to induce blinks (output) is optimized by adding auditory white noise, although the noise alone is not capable of increasing the baseline blink probability. We focus on this situation because dynamical properties of the brain's integration of both auditory and tactile inputs are well identified [14,15]. Based on such properties, we study numerically and analytically an integrate-and-fire (IF) model [16] with short-term synaptic depression (STSD) [17], which nicely accounts for the observed experimental results. We thus suggest this novel class of neural SR constitutes a prominent new mechanism in which neurons in the brain make constructive use of external and/or internal noise, being even applicable in devising noise-assisted, but error-free, signal detectors for weak signals.

The experiment was performed on 46 healthy men (age 18 to 40 yr). Some experimental details and preliminary results were reported by us in Ref. [18]. In this Letter, we present new and additional quantitative data and analysis, which favorably relate to our numerical and analytical theoretical modeling. Tactile stimuli (signals) were applied by air puffs at about 10 mm distance from the lateral canthus. The tactile blink reflexes were detected by an electromyogram (EMG) of the orbicularis oculi muscle, while auditory Gaussian white noise (frequency range 10–20 kHz) was administered through headphones. The threshold of the tactile blink reflex was determined by using a modified up-and-down method [19]. We set the intensity of the tactile stimulation to be 5% below the threshold.

After setting the intensity level, we started sessions to examine response probabilities of the tactile blink reflex at each of the following levels of white auditory noise intensity: 35 [sound pressure level (SPL)], 55, 65, 70, and 85 dB. A search window for the tactile blink reflex was set at 20–100 msec after the onset of the tactile stimulation (see Fig. 1). If the EMG activity exceeded three standard deviations of background activity, which was taken from the corresponding control (no stimulation) trials, we considered a blink response to have occurred [20]. The baseline blink probability (α) per unit (a unit consists of an 80 msec detection window) was taken from the EMG data before each tactile stimulation.

In analyzing these experimental data, we evaluate the detected blink probability β by setting an 80 msec search

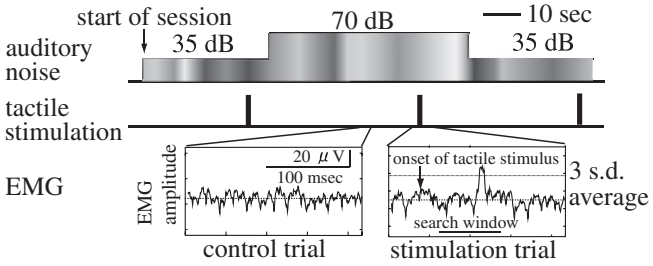

FIG. 1. Diagram of experimental sequences with auditory noise, tactile stimulation, and EMG data within a session (the first three trials are shown) with s.d. denoting standard deviation.

window to count the blink occurrences (Table I) after each tactile stimulation. We assume that the β probability contains baseline blinks at the same probability as α, and then derive the values for the overall tactile blink probability $\gamma = \beta - \alpha$. Consequently, no significant (a level of statistical significance $p > 0.05$) difference in α is detected between sessions. However, Ryan's multiple comparisons reveal that the γ at 70 dB is significantly ($p < 0.05$) higher than those at the other noise levels except for the γ at 65 dB, suggestive of a SR-type optimization of the tactile blink reflex at this intermediate noise intensity.

Both auditory and tactile inputs are known to be integrated in a well-identified region in the brain stem, called the caudal pontine reticular nucleus (PnC), to cause the blink reflex to emerge [14,15]. It is known that few spikes of an auditory neuron can reach the PnC neuron below 55 dB of auditory noise intensity [14]; thus, background noise from other sites in the brain can mainly contribute to an occurrence of the blink reflex at 35 and 55 dB. By contrast, 85 dB auditory noise is considered large enough to elicit an auditory startle reflex [21]. Thus, the membrane potential of PnC neurons can reach the threshold by 85 dB auditory noise alone, and the increase in spike firings should be observed irrespective of the input signals, leading to a corresponding increase in α. This feature, however, is not observed. A synapse which connects to the PnC neuron is known to have adaptive properties [22], where repeated stimulations of the afferent fiber cause a significant decay of the excitatory postsynaptic potential (EPSP). The mechanism at work is proposed to be STSD [23]. Indeed, we demonstrate that our experimental findings are well described by taking such STSD into account.

TABLE I. Experimental findings at differing auditory noise intensities σ. The baseline blink probability within an 80 msec detection window (observed blink numbers/numbers of detection windows) is α; β is the blink probability after tactile stimuli within the search window and γ is the net tactile blink probability. The errors for γ are at 95% confidence level (binominal test). The (*) marks results which are significantly ($p < 0.05$) higher than the remaining ones, with the exception of γ at 65 dB.

σ	α	β	$\gamma = \beta - \alpha$
35 dB (SPL)	34/1912	222/609	0.35 ± 0.04
55 dB	29/1708	40/136	0.28 ± 0.08
65 dB	29/1708	63/150	0.40 ± 0.08
70 dB	40/1721	96/183	0.50 ± 0.08*
85 dB	33/1721	47/138	0.32 ± 0.08

In the PnC neuron, both auditory noise and tactile signals are integrated through synaptic inputs [14,15]. This necessitates the incorporation of the dynamics of the postsynaptic membrane potential into an IF model, being sketched with Fig. 2(a). To this end, we set up an IF model with STSD, describing the dynamics of the postsynaptic membrane potential [16]:

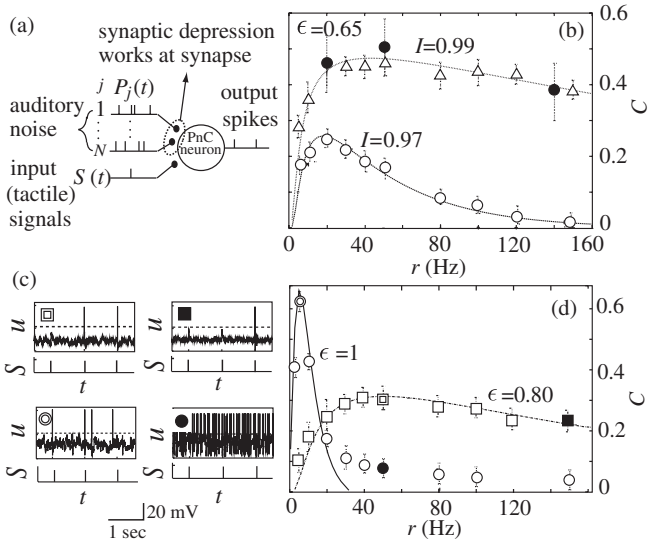

FIG. 2. (a) A schematic diagram of the IF model with input auditory noise, input signals, and output spikes of a PnC neuron. STSD works at the auditory synapse receiving a Poisson spike train. (b) Simulation results for the cross correlation C versus the Poisson rate r for the IF model with implemented STSD. The error bars are standard deviations of 20 trials. The time length of the simulation was 400 sec for each trial. The stimulation interval was 1 sec. Fixed $\epsilon = 0.65$ and $N = 20$ are used. We excluded the first 10 sec of data for transition. n in Eq. (2) for simulation is 9.75×10^4. $I = \eta/(\theta - u_0^\infty)$ represents the relative input signal intensity. The lines are theoretical predictions (see text). The filled circles are experimental data assuming a linear relationship between auditory noise intensities and r (20 Hz for 65 dB and 140 Hz for 85 dB). The error bars for the experimental data represent 95% confidence intervals by the binominal test. (c) Examples of membrane potential fluctuations at corresponding data points in Fig. 2(d). The double square is for $\epsilon = 0.8$ and $r = 40$ (Hz), filled circle for $\epsilon = 1$ and $r = 50$ (Hz), double circle for $\epsilon = 1$ and $r = 5$ (Hz), and the filled square for $\epsilon = 0.8$ and $r = 150$ (Hz). (d) Simulation results for the cross correlation C versus the Poisson rate r with no STSD ($\epsilon = 1$) and $\epsilon = 0.80$. Fixed $N = 50$ is used. The open circles are the results of C for $\epsilon = 1$ [$\eta = 17.6$ (mV)] and the open squares for $\epsilon = 0.80$ ($I = 0.97$).

$$\tau_m \dot{u} = -u + \sum_j^N \omega D_j(t) P_j(t) + S(t), \quad (1)$$

where u is the membrane potential of the PnC neuron and τ_m is the membrane time constant. $S(t)$ is an aperiodic signal given by $S(t) = \eta \sum_n \delta(t - t^{(n)})$, where δ is Dirac's delta function, η is the EPSP amplitude induced by the input signal, and $t^{(n)}$ corresponds to the input time of the tactile stimulation. We take an interval of $S(t)$ to be much longer than τ_m. Thus, we can safely neglect the effects of past aperiodic signals on the present u. $P_j(t)$ is a Poisson spike train (noise) of the jth synapse with the rate r [24]: i.e., $P_j(t) = \sum_n \delta(t - \hat{t}_j^{(n)})$, where $\hat{t}_j^{(n)}$ is the input time of the jth synapse with index n for the nth input. Beyond a startle reflex intensity of ca. 55 dB auditory noise intensity this Poisson firing rate r is directly proportional to the auditory noise intensity σ. ω is a fixed EPSP amplitude of each random synaptic input, and N denotes the total number of synapses with random inputs. If u exceeds the threshold value θ, a spike firing occurs and u is reset to the resting potential u_r, which we set at $u_r = 0$. $D_j(t)$ is a function between 0 and 1 that describes the amount of depression. The initial value $D_j(t = 0)$ is 1. Following the model of STSD by Abbott *et al.* [17], each instant a Poisson spike arrives at synapse j at time $t = \hat{t}^-$, $D_j(t = \hat{t}^+)$ is reduced by multiplicative factor ϵ: $D_j(\hat{t}^+) = \epsilon D_j(\hat{t}^-)$. ($\epsilon$ represents the strength of synaptic depression. Thus, $\epsilon = 1$ implies zero depression and we use $0.65 \leq \epsilon \leq 0.9$.) The recovery dynamics of $D_j(t)$ between successive Poisson inputs is given by $\tau_d \dot{D}_j(t) = 1 - D_j(t)$, where τ_d is the recovery time of depression ($0.2 \leq \tau_d \leq 0.6$ sec).

To measure and to compare the SR effects between experiment and theory, we introduce a normalized input-output cross correlation measure C within the total observation time defined as [25]

$$C = (Z - XY/n)/\sqrt{X(1 - X/n)Y(1 - Y/n)}, \quad (2)$$

where X and Y denote the total numbers of input and output pulses, respectively, and Z is the total number of coincidental firings. The time series is divided into n bins, where the X, Y, and Z take the value of 0 or 1 for each bin. Experimental results in Table I are transformed into C by setting denominators of β to X, numerators of β to Z, denominators of α plus those of β to n, and numerators of β plus those of α are set to Y.

The numerical simulation of Eq. (1) has been performed by using the fourth-order Runge-Kutta method, with $\omega = 2$ (mV), $\tau_m = 0.01$ (sec), $\theta = 20$ (mV), and $\tau_d = 0.6$ (sec) to obtain the r dependence of C. We test this for different signal intensities I [Fig. 2(b)], with the EPSP amplitude η induced by the signals related by $\eta = I(\theta - u_0^\infty)$ where u_0^∞ is $\lim_{r\to\infty} u_0 = N\omega\tau_m/(1 - \epsilon)\tau_d$ [Eq. (4)]. Bell-shaped curves for C against the Poisson firing rate r, hence against the auditory noise intensity, are obtained, being the benchmark behavior of neural SR for this novel class. The experimental data at 65, 70, and 85 dB fit well the simulation results. Furthermore, the results of the simulation are compatible with the experimental results in that the firing rate in the absence of signals, or the error rate f in Fig. 3(b), does not increase with increasing r when STSD is sufficiently at work, i.e., for $\epsilon < 0.9$.

Analytical results can be obtained as well. To start with, we set $\bar{D}^n = D_j(\hat{t}_j^{(n)})$, where $\bar{D}^n$ corresponds to the value of $D_j(t)$ just before the nth synaptic input, to obtain the recurrence equation for $\bar{D}^n$, i.e.,

$$\bar{D}^n = 1 - (1 - \epsilon\bar{D}^{n-1})\hat{g}, \quad (3)$$

where $\hat{g} = \exp(-\hat{t}_j^{(n)}/\tau_d)$. For $n \to \infty$, the expectation value of the amplitude of each synaptic input is given by $\omega\langle\bar{D}^\infty\rangle = \omega/[1 + (1 - \epsilon)\tau_d r]$. Let us next consider the dynamics in the absence of a threshold and the external signal $S(t)$ to obtain the mean potential shift u_0 and the variance of membrane potential fluctuations due to pure Poisson spike inputs. The stationary membrane potential fluctuations u are given by $u(t) = \sum_j^N \omega \int_0^\infty D_j(t - s)v(s)P_j(t - s)ds$, where $v(s) = \exp(-s/\tau_m)$. The mean potential is $u_0 = \langle u\rangle$, where $\langle\cdot\rangle$ denotes a statistical average, and the variance $\langle\Delta u^2\rangle = \langle[u(t) - u_0]^2\rangle$ reads

$$u_0 = \omega N r \tau_m/[1 + (1 - \epsilon)\tau_d r], \quad (4)$$

$$\langle\Delta u^2\rangle \simeq 0.5 N r \omega^2 \tau_m \langle(\bar{D}^n)^2\rangle. \quad (5)$$

From Eq. (3), we can evaluate the steady-state expectation value $\lim_{n\to\infty}\langle(\bar{D}^n)^2\rangle$, to yield for the variance

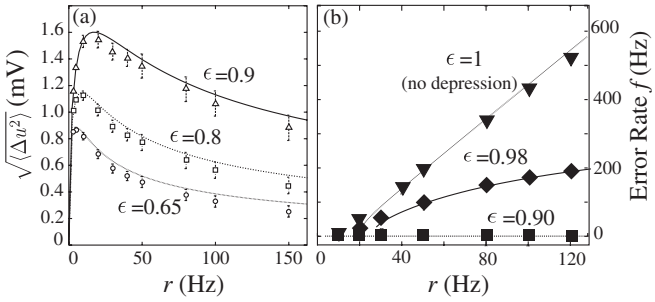

FIG. 3. (a) Simulation results for the membrane potential fluctuation $\sqrt{\langle\Delta u^2\rangle}$ versus the Poisson rate r. The error bars are standard deviations for 10 trials. The total simulation time of each trial was 40 sec. The time step of the simulation was 0.1 msec. Membrane fluctuation data are collected from the last 10 sec of the simulation results. The lines are the theoretical predictions for each ϵ from Eq. (6). (b) Error firing rates f (Hz), i.e., the firing rates in the absence of the signals $S(t)$ versus the Poisson firing rate r for different ϵ. The filled triangles are for $\epsilon = 1$, filled oblique squares for $\epsilon = 0.98$, and filled squares for $\epsilon = 0.9$. The lines denote the analytical predictions. We used $f = f^+(\theta)$ if $u_0 > \theta$ (for $\epsilon = 1$ and $\epsilon = 0.98$) and $f = f^-(\theta)$ if $u_0 < \theta$ (for $\epsilon = 0.90$).

$$\langle \Delta u^2 \rangle \simeq Nr\omega^2\tau_m/\{[2 + (1 - \epsilon^2)r\tau_d][1 + (1 - \epsilon)r\tau_d]\}. \quad (6)$$

The dependence of $\sqrt{\langle \Delta u^2 \rangle}$ on the Poisson rate r fits well with the numerical simulation results [Fig. 3(a)], suggesting that a larger Poisson rate, and thus a larger external noise intensity, causes decreasing membrane voltage fluctuations which in turn determine the baseline firing rates, i.e., the baseline blink probability α in the experiment.

From Eqs. (4) and (6), and the firing rate of an IF model for $u_0 < \theta$ [12], i.e.,

$$f^-(\theta) \simeq (c/\tau_m) \exp(-[u_0 - \theta]^2/2\langle \Delta u^2 \rangle), \quad (7)$$

where c is a constant, we can evaluate the SR curves analytically. The index $^-$ is used for $f(\theta)$ when u_0 is in the subthreshold region. For $u_0 \gg \theta$, the firing rate $f^+(\theta)$ is given by $f^+(\theta) \simeq -1/[\tau_m \ln(1 - \theta/u_0)]$ [26]. Assuming $u_0 < \theta$, the value of coincidental firing Z_c within the time window Δ is given by $Z_c \simeq \Delta f^-(\theta - \eta)$. Upon setting the total observation time to t_k and the total number of signals to X, the value of the total output spikes Y is given by $Y = XZ_c + t_k f^-(\theta)$ and the total coincidental firings Z is given by XZ_c. Combining these results with Eq. (2) yields the theoretical predictions for C, which very nicely fit our simulation data with $c = 1.3$ at different relative intensities I [Fig. 2(b)] and ϵ [Fig. 2(d)]. As shown with Fig. 2(d), C for $\epsilon = 1$ starts to decrease due to an increment of error rate f. In clear contrast, with STSD at work, there occurs no firing in the absence of signals with the error firing rates $f^-(\theta) \approx 0$ [Fig. 3(b)] for all r. A neuron with sufficient STSD can fire only when subthreshold signals arrive [Fig. 2(c), upper] and, even with the error rate f being zero, the neuron with STSD can display SR-type behavior. Consequently, the neuron with STSD can act as an error-free detector for weak signals.

In summary, we have explored experimentally and theoretically a novel class of neural SR in the auditory noise-optimized human tactile blink reflex. An IF model with STSD nicely accounts for the experimental findings. The novelty of this class of SR lies in the fact that the dropoff of the input-output cross correlation C at large auditory noise intensity (or Poisson rates r) arises without an increase in noise-induced random firings. This very feature is in distinct contrast to conventional SR, where the corresponding escape rates monotonically increase with increasing noise intensity [2]. This novel feature enables a neuron to act as an error-free detector for weak signals. Within our experimental framework, this means that humans can react to weak tactile signals by making use of auditory noise but without being disturbed by too much auditory noise. We thus conclude that this class of neural SR provides yet another important mechanism by which neurons in the brain operate in noisy internal or external environments. The development of synthetic detectors based upon such a mechanism may prove to be of considerable practical value as well.

This work was partly supported by grants from the Japan Society for the Promotion of Science for Young Scientists (T. M.).

*yamamoto@p.u-tokyo.ac.jp

[1] K. Wiesenfeld and F. Moss, Nature (London) **373**, 33 (1995).
[2] L. Gammaitoni *et al.*, Rev. Mod. Phys. **70**, 223 (1998).
[3] P. Hänggi, Chem. Phys. Chem. **3**, 285 (2002).
[4] J. K. Douglass *et al.*, Nature (London) **365**, 337 (1993).
[5] J. J. Collins *et al.*, J. Neurophysiol. **76**, 642 (1996).
[6] J. E. Levin and J. P. Miller, Nature (London) **380**, 165 (1996).
[7] D. Nozaki *et al.*, Phys. Rev. Lett. **82**, 2402 (1999).
[8] J. J. Collins *et al.*, Nature (London) **383**, 770 (1996).
[9] I. Hidaka *et al.*, Phys. Rev. Lett. **85**, 3740 (2000).
[10] K. Kitajo *et al.*, Phys. Rev. Lett. **90**, 218103 (2003).
[11] R. Soma *et al.*, Phys. Rev. Lett. **91**, 078101 (2003).
[12] H. E. Plesser and W. Gerstner, Neural Comput. **12**, 367 (2000).
[13] D. Nozaki *et al.*, Phys. Rev. E **60**, 4637 (1999).
[14] K. Lingenhöhl and E. Friauf, J. Neurosci. **14**, 1176 (1994).
[15] J. S. Yeomens *et al.*, Neurosci. Biobehav. Rev. **26**, 1 (2002).
[16] R. B. Stein, Biophys. J. **5**, 173 (1965).
[17] L. F. Abbott *et al.*, Science **275**, 220 (1997).
[18] H. Yasuda *et al.*, in *Noise and Fluctuations*, edited by M. Tacano *et al.* (American Institute of Physics, New York, 2007), pp. 545–548.
[19] W. J. Dixon and A. Mood, J. Am. Stat. Assoc. **43**, 109 (1948).
[20] E. M. Ornitz *et al.*, Clin. Neurophysiol. **112**, 2209 (2001).
[21] K. M. Berg, Ph.D. thesis, University of Wisconsin, 1973.
[22] M. Koch, Prog. Neurobiol. **59**, 107 (1999).
[23] M. Weber *et al.*, Eur. J. Neurosci. **16**, 1325 (2002).
[24] W. Gerstner and W. M. Kistler, *Spiking Neuron Models* (Cambridge University Press, Cambridge, 2002).
[25] G. Palm *et al.*, Biol. Cybern. **59**, 1 (1988).
[26] H. C. Tuckwell, *Introduction to Theoretical Neurobiology* (Cambridge University Press, Cambridge, 1988), Vol. 2.